THE JOURNAL OF PHYSICAL CHEMISTRY C

Article

Cite This: J. Phys. Chem. C 2018, 122, 17118−17122

pubs.acs.org/JPCC

Computational Design of Two-Dimensional Perovskites with Functional Organic Cations

Sudeep Maheshwari, Tom J. Savenije, Nicolas Renaud, and Ferdinand C. Grozema*

Department of Chemical Engineering, Delft University of Technology, Delft 2629, The Netherlands

ABSTRACT: Two-dimensional (2D) halide perovskites are a class of materials in which 2D layers of perovskite are separated by large organic cations. Conventionally, the 2D perovskites incorporate organic cations as spacers, but these organic cations also offer a route to introduce specific functionality in the material. In this work, we demonstrate, by density functional theory calculations, that the introduction of electron withdrawing and electron donating molecules leads to the formation of localized states, either in the organic or the inorganic part. Furthermore, we show that the energy of the bands located in the organic and inorganic parts can be tuned independently. The organic cation levels can be tuned by changing the electron withdrawing/donating character, whereas the energy levels in the inorganic part can be modified by varying the number of inorganic perovskite layers. This opens a new window for the design of 2D perovskites with properties tuned for specific applications.

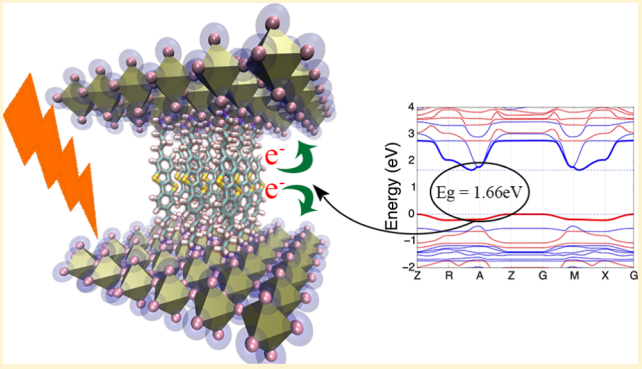

INTRODUCTION

The two-dimensional (2D) versions of hybrid halide perovskites are an emerging class of opto-electronic materials displaying robust environmental stability as compared to their three-dimensional (3D) counterparts.[1] These materials have not been studied as extensively as the 3D equivalents, but they have been considered for applications such as photodetectors,[2] lasers,[3] field effect transistors,[4] and light emitting devices.[4,5] They structurally differ from the 3D perovskites because the organic cation in these materials is not limited in size by the Goldschmidt tolerance factor. This allows for the introduction of a wider choice of bulkier organic cations, including aromatic and divalent ones. Previous theoretical studies on the 2D perovskites with varying organic cations have predicted that a change in the structure of the organic cation can result in a modulation of the steric effects, electronic structure, and electronic properties of the material.[6] In a separate study with similar systems, it was shown that the 2D perovskites assume similar effective masses for the charge carriers in both valence and conduction bands.[7]

Two-dimensional (2D) AM_2X_4 or BMX_4 perovskites consists of bulky monovalent cation A^+ or divalent cation B^{2+} as the organic component. MX_4 is the tetrahalogenide or inorganic component of the material consisting for instance of Pb^{2+} (M) and I^- (X) atoms. The basic crystal packing of these hybrid materials is a self-assembled, layered structure where single sheets of corner shared MX_6 octahedra and bilayers of organic cations are stacked alternately, held together by Coulombic and van der Waals forces.[8] The interest in these materials is not new as their quantum-well structure has been studied for over two decades. In 1988, Goto and co-workers first reported a high exciton binding energy for one such material. The exciton binding energy for $(CH_{10}N_{21}H_3)_2PbI_4$ was found to be 10 times higher than that of PbI_2.[9] This difference was attributed to the 2D character of the exciton and the small dielectric constant of the long alkyl chains. The 2D perovskites also display much more efficient photoluminescence than their three-dimensional counterparts because of the existence of bound excitons in the metal halide sheets. The quantum and dielectric confinement due to the organic cation strongly affects the exciton binding energy of the material, which is generally in the range of 200−300 meV.[10] Therefore, the charge carriers in these materials primarily exist in the form of bound excitons at room temperature.[11] The chemical and physical properties of 2D perovskites are highly tunable as compared to those of its 3D counterpart. This is because the layer thickness of the 2D sheets can be modulated by introducing organic cations of different size.[12,13]

When the monovalent large organic cations are mixed with the small cations like methylammonium and formamidinium, which are generally used to form 3D perovskites, it is possible to create so-called Ruddlesden−Popper phases of hybrid perovskites. The divalent large organic cations on the other hand form Dion−Jacobson 2D perovskites which were recently developed by Mao et al. with composition of aminomethylpiperidinium organic cations.[14] Within both Ruddlesden−Popper and Dion−Jacobson perovskite structures, the inorganic layers incorporate smaller organic cations and are

Received: June 14, 2018
Revised: July 6, 2018
Published: July 8, 2018

DOI: 10.1021/acs.jpcc.8b05715
J. Phys. Chem. C 2018, 122, 17118−17122

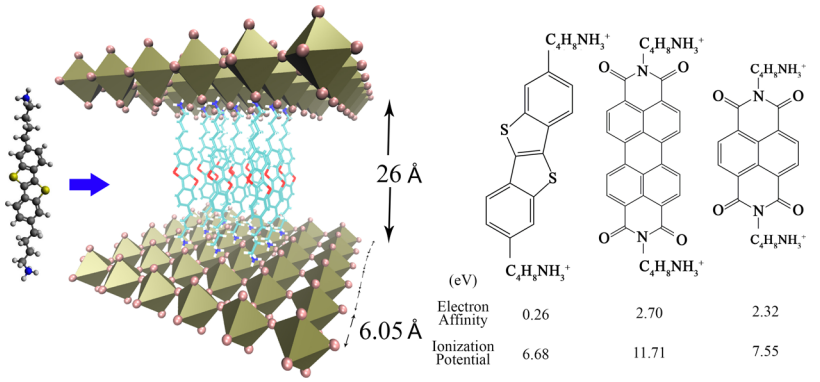

Figure 1. $(n\text{Bu}-\text{NH}_3)_2\text{BTBT}$ as the organic molecule between the inorganic sheets of with PbI_4 layer depicting Pb−Pb distance as 6.05 Å and the interlayer distance as 26 Å. The molecular structure of BTBT, PDI, and NDI functional organic molecules and their electron affinity and ionization potential values.

separated from each other through spacers of the bulky organic cations.[13−15] These quasi-2D materials have been demonstrated to be useful as the active material in photovoltaic cells, albeit with considerably lower efficiency than their fully 3D counterpart.[13,16] We have recently shown that the exciton binding energy strongly depends on the number of inorganic layers in between the bulky organic cations. The binding energy was found to decrease from 370 meV for the purely 2D materials to 80 meV for a material with four inorganic lead iodide layers between the organic part.[17] This shows that modifications in the number of inorganic layers do not only affect the band gap of the material but also affect the efficiency of charge generation.

Until now, most of the bulky organic cations used in 2D or quasi-2D perovskite materials mainly contribute in defining the physical attributes of the material including dimensionality of the system and their phase behavior.[18,19] These organic cations have a large HOMO−LUMO gap and thus the electronic properties of the resulting materials is fully determined by the properties of the inorganic layers.[20] In this work, we aim to introduce new designs for the 2D layered perovskites by incorporating unconventional organic cations between the inorganic layers of lead iodide. We have investigated the electronic structure of these 2D and quasi-2D perovskites where the organic cations as strong electron donor and acceptor are introduced. We show that this leads to either valence band maxima or conduction band minima that are localized in the organic spacer layer. The positioning of these localized bands with respect to the bands in the inorganic part can be tuned by introducing additional electron donating or electron withdrawing substituents. Such materials are expected to exhibit enhanced formation of free charges upon photoexcitation, even for pure 2D systems where the exciton binding energy is very high.

COMPUTATIONAL METHODS

We have investigated the electronic structure and charge transport properties of 2D perovskites in which the organic cation contains 2,7-dibutylammonium[1]benzothieno[3,2-*b*]-[1]benzothiophene (BTBT), *N*,*N*-bis(*n*-butylammonium)-perylene-3,4,9,10-tetracarboxylic diimide (PDI), and *N*,*N*-bis(*n*-butylammonium)naphthalene-1,4,5,8-tetracarboxylic diimide (NDI) chromophores as the functional component. These organic chromophores are well-known from organic electronics and offer a chance to combine the properties of perovskites and organic semiconductors.[21−24] The optimization of the $X-PbI_4$ structures was performed using projector augmented wave pseudopotentials with van der Waals corrected Perdew−Burke−Ernzerhof−sol exchange correlation functional as implemented in VASP 5.4.1.[25−30] Relativistic effects were included fully for the core electrons for each atom, and the scalar relativistic approximation was applied for the valence electrons. An energy cutoff of 500 eV and a gamma-centered Brillouin zone sampling grid of 4 × 4 × 2 were chosen for the calculations. The ionic positions were relaxed while conserving the tetragonal lattice shape for continuous values of lattice parameter. Band structures of the different $X-PbI_4$ geometries were then computed at the density functional theory (DFT) level of theory at a denser mesh in the direction of high symmetry.

RESULTS AND DISCUSSION

To introduce organic cations with added functionality to the 2D perovskite materials, we have chosen electron donating and electron withdrawing compounds that are well-known from organic electronics. We have performed DFT calculations on 2D sheets of lead iodide where conjugated chromophores with ammonium groups coupled by alkyl linker are introduced. The structure of these organic cations together with their electron affinity and ionization potential values are shown in Figure 1. As seen in this figure, the electron affinity is high for the electron acceptor molecules PDI and NDI and much smaller for the electron donor molecule BTBT. The ionization potential is lowest for BTBT and higher for the electron acceptors PDI and NDI. The geometry optimization of $X-PbI_4$, where X refers to the functional organic cation, was performed to obtain the lattice constants for a tetragonal lattice. The system with electron donating cation X = $(n\text{Bu}-\text{NH}_3)_2\text{BTBT}$ is referred to as BTBT further. The optimized geometry for BTBT assumes a unit cell with lattice parameters a = 6.05 Å and c = 26.00 Å as shown in Figure 1 and reported in Table 1. Here, a corresponds to the in-plane distance between the neighboring lead atoms and c corresponds to the distance between the planes of the inorganic sheets of lead iodide. The lattice constant a is smaller as compared to that of the reported Ruddlesden−Popper phase 2D perovskites with butylammonium as the organic cation and having Pb−Pb distance of 6.216 Å.[15] A smaller distance between the lead and iodide atoms in the inorganic sheet ensures stronger coupling between neighboring atoms, leading to improved charge

DOI: 10.1021/acs.jpcc.8b05715
J. Phys. Chem. C 2018, 122, 17118−17122

Table 1. Lattice Constants for the Tetragonal Unit Cell of the Optimized Geometry of X−PbI_4, where X = (nBu−NH_3)$_2$BTBT, X = (nBu−NH_3)$_2$PDI and X = (nBu−NH_3)$_2$NDI

	BTBT	PDI	NDI
a (Å)	6.05	6.05	6.05
c (Å)	26.00	28.00	23.7

transport. The band structure computed for the optimized geometry of BTBT is shown in the Figure 2a. It is plotted with

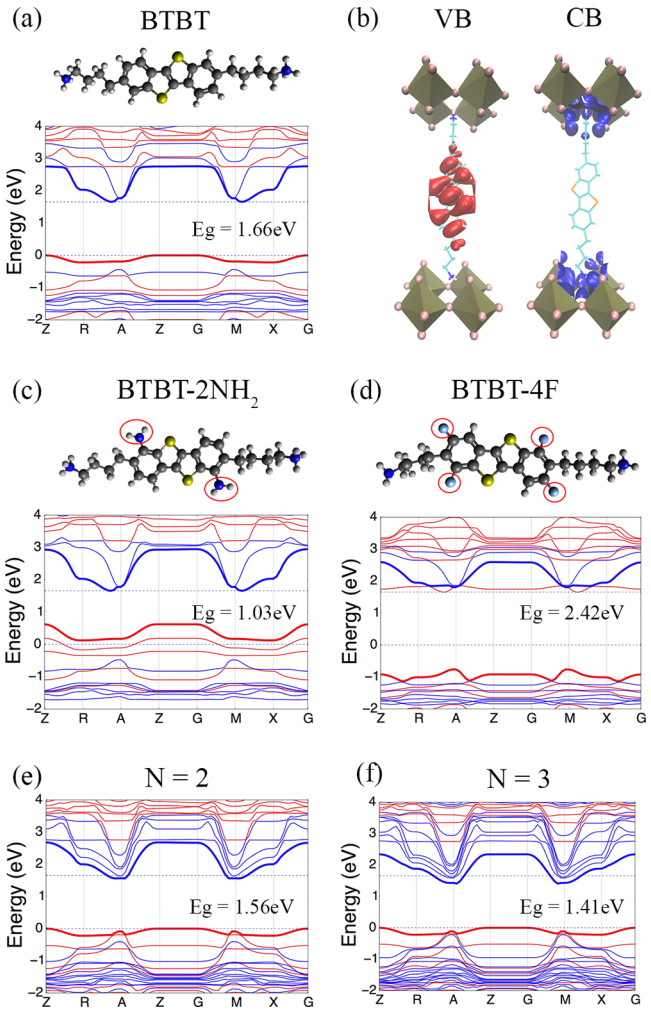

Figure 2. (a) Band structure of optimized geometry of X−PbI_4 where X = (nBu−NH_3)$_2$BTBT. The bands in blue are localized on pbI_4 sheets whereas bands in red are localized on the organic cation. (b) Band-decomposed charge density for valence band maximum and conduction band minimum for BTBT. (c) Band structure for −NH_2 substitution on BTBT. (d) Band structure for −F substitution on BTBT. (e) Band structure for n = 2 in (nBu−NH_3)$_2$BTBTPb_nI_{3n+1}. (f) Band structure for n = 3 in (nBu−NH_3)$_2$BTBTPb_nI_{3n+1}.

different colors for the bands located on the organic molecule and the lead iodide perovskite sheet. A band gap of 1.66 eV is obtained for this system, close to the band gap for methylammonium lead iodide.[31] The value of the band gap is considerably lower than that of the single-layer lead iodide perovskite with butylammonium as the organic cation and shows the effect of the organic cation on the band gap tunability of the 2D system of lead iodide.[15] To visualize the valence band maximum and conduction band minimum, a band-decomposed charge density was extracted as shown in Figure 2b. The highest valence band for BTBT is localized on the aromatic core of organic cation, whereas the lowest conduction band is localized on the lead iodide layers. This clearly shows that BTBT acts as a donor of electrons in this organic−inorganic system of 2D perovskites.

The electron donating nature of the organic molecule can be modified by introduction of electron donating(−NH_2) and withdrawing(−F) groups on the aromatic core, see Figure 2c,d. The substitution of electron donating −NH_2 groups leads to a shift of the bands localized on the organic cation to higher energy whereas substitution of −F groups leads to the shift of the bands of the organic cation to lower energy. These substitutions have a negligible effect on the position of the perovskite bands. The band gap of the system decreases to 1.03 eV with electron donating amine groups, whereas fluorides lead to increase in the band gap to 2.42 eV. This shows that the bands localized on the organic part of the material can be modified, independent of the band on the inorganic part. Similarly, we can modify the electronic structure of the inorganic part by changing the number of inorganic layers. We have computed the band structure for Ruddlesden−Popper structure with multiple layers of perovskite (N = 2 and N = 3) in between the organic layers. The band structures for these materials are shown in Figure 2e,f. The band gap of the system decreases with the increasing perovskite layers which is 1.56 eV for N = 2 and 1.41 eV for N = 3. This is caused by a movement of the conduction bands, localized on the inorganic part, to lower energies.

To study the effect of the introduction of electron withdrawing groups, the cations X = (nBu−NH_3)$_2$PDI and (nBu−NH_3)$_2$NDI (referred to as PDI and NDI) were considered. The optimized lattice constants for both of these compounds are reported in Table 1. The in-plane Pb−Pb distance is the same for all three structures investigated, indicating that changes in the core of the organic cation have only a small effect on the distance between the lead atoms in the 2D inorganic sheets. In the optimized geometry for PDI and NDI molecules, π-stacked structures can be observed. Such π-stacking was not observed for BTBT because of the smaller size of its core. The formation of π-stacks is important in these systems, as it can introduce pathway for charge transport through the organic layers. The band structures computed for the optimized geometry of PDI−PbI_4 and NDI−PbI_4 are shown in Figure 3. The band gap of these systems is much lower than for the BTBT system, 0.11 and 0.32 eV, respectively. A band decomposition of the charge density for the PDI and NDI systems shows that the highest valence band is localized on the lead iodide layer, whereas the lowest conduction band is localized on aromatic core of the organic molecule. This is opposite to what was observed for the electron donating BTBT cation above.

To gain insights into the charge transport properties of these systems with electron donors and acceptor, the effective masses were calculated by a band fitting method for the highest valence band and lowest conduction band for the various combinations of organic cations with lead iodide sheets in Table 2. The effective masses within the 2D sheet are lower than those perpendicular to the sheet in all cases. This indicates, as expected, that transport perpendicular to the inorganic layers is very inefficient as compared to the in-plane transport. For the 2D system with BTBT, the effective mass of

DOI: 10.1021/acs.jpcc.8b05715
J. Phys. Chem. C 2018, 122, 17118−17122

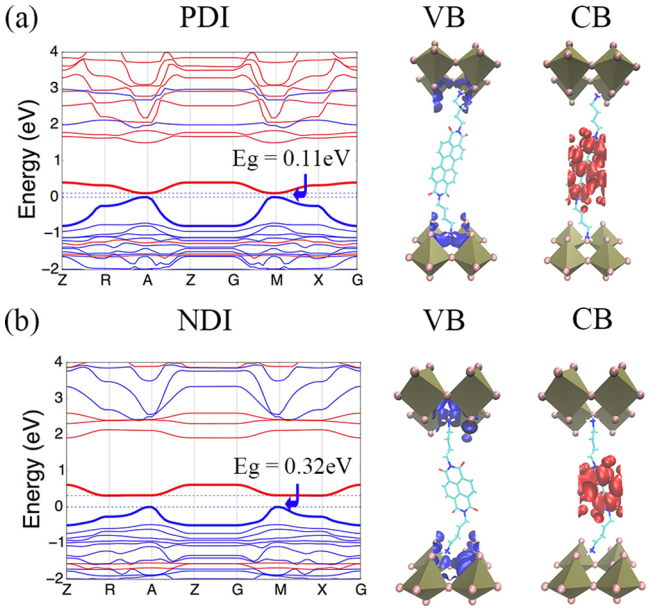

Figure 3. (a) Band structure of optimized geometry of $(n\text{Bu}-NH_3)_2PDIPbI_4$. The bands in blue depicting contribution from the inorganic PbI_4 whereas bands in red depicting contribution from $(n\text{Bu}-NH_3)_2PDI$. (b) Band structure of optimized geometry of $(n\text{Bu}-NH_3)_2NDIPbI_4$. The bands in blue depicting contribution from the inorganic PbI_4, whereas bands in red depicting contribution from $(n\text{Bu}-NH_3)_2NDI$. Band decomposed charge density for valence band maximum and conduction band minimum can be seen with each band structure.

the electrons is 0.12 which is much lower compared with the effective mass for holes which is 3.88. This is because of the localization of the respective bands. The electrons are in the inorganic layers where they can move easily, whereas the holes are in the BTBT layer where transport relies on coupling between the different molecules that are relatively far apart. For PDI and NDI, the effective masses are opposite to those for BTBT and the hole mass is lower than the electron mass. As shown above, in PDI and NDI, the hole is localized in the inorganic layer where it can move freely, whereas the electrons are on the organic part where transport relies on $\pi-\pi$-interaction between neighboring molecules. The electronic structure of these materials is considerably different from those previously published for 2D Ruddlesden–Popper phases containing butylammonium as the organic cation spacers. The effective masses for both electrons and holes in these phases are in the range of $0.08m_e-0.14m_e$. Also, the organic cations here do not participate in charge transport.[13] Thus, the inclusion of novel organic cations in organic layers offers a possibility to improve the charge transport in the organic part by engineering the π-stacking in this layer.

In conclusion, we have performed a DFT-based study of 2D hybrid perovskites, where functional organic cations are incorporated that have strongly electron donating or withdrawing capacities. We show that the energies of these organic molecules can be such that either the valence band or the conduction band becomes localized on the organic part of the material. This is stark contrast to the commonly used organic cations that only serve as a spacer layer that does not affect the electronic properties. We also show that it is possible to tune the alignment of the energy levels in the organic part by introducing additional donating and accepting groups such as amines or fluorines. This tuning leaves the band energies in the inorganic part unaffected. A similar tuning can be done in the inorganic part by varying the number of inorganic perovskite layers between the organic part of the materials. These results illustrate that the properties of 2D halide perovskites can be tuned by the introduction of functional organic units. This offers a new approach for tuning the properties of these materials to develop stable 2D perovskites with specific functionality, for instance, improved charge separation for photovoltaic applications.

AUTHOR INFORMATION

Corresponding Author

*E-mail: f.c.grozema@tudelft.nl.

ORCID

Tom J. Savenije: 0000-0003-1435-9885

Ferdinand C. Grozema: 0000-0002-4375-799X

Notes

The authors declare no competing financial interest.

ACKNOWLEDGMENTS

This work is part of an Industrial Partnership Programme of the Foundation for Fundamental Research on Matter (FOM), which is part of the Netherlands Organisation for Scientific Research (NWO). The research leading to these results in the Delft University of Technology has received funding from the European Research Council Horizon 2020 ERC grant agreement no. 648433.

REFERENCES

(1) Smith, I. C.; Hoke, E. T.; Solis-Ibarra, D.; McGehee, M. D.; Karunadasa, H. I. A Layered Hybrid Perovskite Solar-Cell Absorber with Enhanced Moisture Stability. *Angew. Chem.* **2014**, *126*, 11414–11417.

(2) Dou, L.; Wong, A. B.; Yu, Y.; Lai, M.; Kornienko, N.; Eaton, S. W.; Fu, A.; Bischak, C. G.; Ma, J.; Ding, T.; Ginsberg, N. S.; Wang, L.-W.; Alivisatos, A. P.; Yang, P. Atomically thin two-dimensional organic-inorganic hybrid perovskites. *Science* **2015**, *349*, 1518–1521.

(3) Deschler, F.; Price, M.; Pathak, S.; Klintberg, L. E.; Jarausch, D.-D.; Higler, R.; Hüttner, S.; Leijtens, T.; Stranks, S. D.; Snaith, H. J.; Atatüre, M.; Phillips, R. T.; Friend, R. H. High photoluminescence efficiency and optically pumped lasing in solution-processed mixed halide perovskite semiconductors. *J. Phys. Chem. Lett.* **2014**, *5*, 1421–1426.

(4) Kagan, C. R.; Mitzi, D. B.; Dimitrakopoulos, C. D. Organic-inorganic hybrid materials as semiconducting channels in thin-film field-effect transistors. *Science* **1999**, *286*, 945–947.

Table 2. Effective Mass of Electrons and Holes for BTBT, PDI, and NDI within the 2D Sheets and Perpendicular to the Sheets

	BTBT		PDI		NDI	
	m_h^*	m_e^*	m_h^*	m_e^*	m_h^*	m_e^*
within sheets	3.88	0.12	0.32	7.83	0.24	1.83
perpendicular to sheets	209.9	293.1	64.5	49.3	21.7	27.7

DOI: 10.1021/acs.jpcc.8b05715
J. Phys. Chem. C 2018, 122, 17118–17122

(5) Tan, Z.-K.; Moghaddam, R. S.; Lai, M. L.; Docampo, P.; Higler, R.; Deschler, F.; Price, M.; Sadhanala, A.; Pazos, L. M.; Credgington, D.; Hanusch, F.; Bein, T.; Snaith, H. J.; Friend, R. H. Bright light-emitting diodes based on organometal halide perovskite. *Nat. Nanotechnol.* **2014**, *9*, 687−692.
(6) Fraccarollo, A.; Cantatore, V.; Boschetto, G.; Marchese, L.; Cossi, M. Ab initio modeling of 2D layered organohalide lead perovskites. *J. Chem. Phys.* **2016**, *144*, 164701.
(7) Pedesseau, L.; Sapori, D.; Traore, B.; Robles, R.; Fang, H.-H.; Loi, M. A.; Tsai, H.; Nie, W.; Blancon, J.-C.; Neukirch, A.; Tretiak, S.; Mohite, A. D.; Katan, C.; Even, J.; Kepenekian, M. Advances and promises of layered halide hybrid perovskite semiconductors. *ACS Nano* **2016**, *10*, 9776−9786.
(8) Ahmad, S.; Kanaujia, P. K.; Beeson, H. J.; Abate, A.; Deschler, F.; Credgington, D.; Steiner, U.; Prakash, G. V.; Baumberg, J. J. Strong photocurrent from two-dimensional excitons in solution-processed stacked perovskite semiconductor sheets. *ACS Appl. Mater. Interfaces* **2015**, *7*, 25227−25236.
(9) Ishihara, T.; Takahashi, J.; Goto, T. Exciton state in two-dimensional perovskite semiconductor (C10H21NH3)2PbI410H 21NH 3 2PbI 4. *Solid State Commun.* **1989**, *69*, 933−936.
(10) Muljarov, E. A.; Tikhodeev, S. G.; Gippius, N. A.; Ishihara, T. Excitons in self-organized semiconductor/insulator superlattices: PbI-based perovskite compounds. *Phys. Rev. B: Condens. Matter Mater. Phys.* **1995**, *51*, 14370−14378.
(11) Chen, Y.; Sun, Y.; Peng, J.; Tang, J.; Zheng, K.; Liang, Z. 2D RuddlesdenPopper perovskites for optoelectronics. *Adv. Mater.* **2018**, *30*, 1703487.
(12) Rodríguez-Romero, J.; Hames, B. C.; Mora-Seró, I.; Barea, E. M. Conjugated organic cations to improve the optoelectronic properties of 2D/3D perovskites. *ACS Energy Lett.* **2017**, *2*, 1969−1970.
(13) Stoumpos, C. C.; Cao, D. H.; Clark, D. J.; Young, J.; Rondinelli, J. M.; Jang, J. I.; Hupp, J. T.; Kanatzidis, M. G. Ruddlesden-Popper Hybrid Lead Iodide Perovskite 2D Homologous Semiconductors. *Chem. Mater.* **2016**, *28*, 2852−2867.
(14) Mao, L.; Ke, W.; Pedesseau, L.; Wu, Y.; Katan, C.; Even, J.; Wasielewski, M. R.; Stoumpos, C. C.; Kanatzidis, M. G. Hybrid Dion-Jacobson 2D Lead Iodide Perovskites. *J. Am. Chem. Soc.* **2018**, *140*, 3775−3783.
(15) Cao, D. H.; Stoumpos, C. C.; Farha, O. K.; Hupp, J. T.; Kanatzidis, M. G. 2D homologous perovskites as light-absorbing materials for solar cell applications. *J. Am. Chem. Soc.* **2015**, *137*, 7843−7850.
(16) Tsai, H.; et al. High-efficiency two-dimensional Ruddlesden-Popper perovskite solar cells. *Nature* **2016**, *536*, 312−316.
(17) Gélvez-Rueda, M. C.; Hutter, E. M.; Cao, D. H.; Renaud, N.; Stoumpos, C. C.; Hupp, J. T.; Savenije, T. J.; Kanatzidis, M. G.; Grozema, F. C. Interconversion between free charges and bound excitons in 2D hybrid lead halide perovskites. *J. Phys. Chem. C* **2017**, *121*, 26566−26574.
(18) Needham, G. F.; Willett, R. D.; Franzen, H. F. Phase transitions in crystalline models of bilayers. 1. Differential scanning calorimetric and x-ray studies of (C12H25NH3)2MCl4 and (NH3C14H29NH3)-2MCl4 salts (M = Mn2+, Cd2+, Cu2+). *J. Phys. Chem.* **1984**, *88*, 674−680.
(19) Saparov, B.; Mitzi, D. B. Organic-Inorganic Perovskites: Structural Versatility for Functional Materials Design. *Chem. Rev.* **2016**, *116*, 4558−4596.
(20) Mitzi, D. B.; Chondroudis, K.; Kagan, C. R. Design, Structure, and Optical Properties of Organic−Inorganic Perovskites Containing an Oligothiophene Chromophore. *Inorg. Chem.* **1999**, *38*, 6246−6256.
(21) Ebata, H.; Izawa, T.; Miyazaki, E.; Takimiya, K.; Ikeda, M.; Kuwabara, H.; Yui, T. Highly soluble [1]Benzothieno[3,2-b]-benzothiophene (BTBT) derivatives for high-performance, solution-processed organic field-effect transistors. *J. Am. Chem. Soc.* **2007**, *129*, 15732−15733.
(22) Yang, J.; Xiao, B.; Tajima, K.; Nakano, M.; Takimiya, K.; Tang, A.; Zhou, E. Comparison among Perylene Diimide (PDI), Naphthalene Diimide (NDI), and Naphthodithiophene Diimide (NDTI) Based n-Type Polymers for All-Polymer Solar Cells Application. *Macromolecules* **2017**, *50*, 3179−3185.
(23) Marcon, V.; Breiby, D. W.; Pisula, W.; Dahl, J.; Kirkpatrick, J.; Patwardhan, S.; Grozema, F.; Andrienko, D. Understanding Structure−Mobility Relations for Perylene Tetracarboxydiimide Derivatives. *J. Am. Chem. Soc.* **2009**, *131*, 11426−11432.
(24) Herbst, W.; Hunger, K.; Wilker, G.; Ohleier, H.; Winter, R. *Industrial Organic Pigments: Production, Properties, Applications*, 3rd Edition; Wiley, 2005.
(25) Blöchl, P. E. Projector augmented-wave method. *Phys. Rev. B: Condens. Matter Mater. Phys.* **1994**, *50*, 17953−17979.
(26) Kresse, G.; Joubert, D. From ultrasoft pseudopotentials to the projector augmented-wave method. *Phys. Rev. B: Condens. Matter Mater. Phys.* **1999**, *59*, 1758−1775.
(27) Grimme, S.; Antony, J.; Ehrlich, S.; Krieg, H. A consistent and accurate ab initio parametrization of density functional dispersion correction (DFT-D) for the 94 elements H-Pu. *J. Chem. Phys.* **2010**, *132*, 154104.
(28) Perdew, J. P.; Burke, K.; Ernzerhof, M. Generalized gradient approximation made simple [Phys. Rev. Lett. 77, 3865 (1996)]. *Phys. Rev. Lett.* **1997**, *78*, 1396.
(29) Perdew, J. P.; Burke, K.; Ernzerhof, M. Generalized gradient approximation made simple. *Phys. Rev. Lett.* **1996**, *77*, 3865−3868.
(30) Perdew, J. P.; Ruzsinszky, A.; Csonka, G. I.; Vydrov, O. A.; Scuseria, G. E.; Constantin, L. A.; Zhou, X.; Burke, K. Restoring the density-gradient expansion for exchange in solids and surfaces. *Phys. Rev. Lett.* **2008**, *100*, 136406.
(31) Eperon, G. E.; Stranks, S. D.; Menelaou, C.; Johnston, M. B.; Herz, L. M.; Snaith, H. J. Formamidinium lead trihalide: a broadly tunable perovskite for efficient planar heterojunction solar cells. *Energy Environ. Sci.* **2014**, *7*, 982−988.

DOI: 10.1021/acs.jpcc.8b05715
J. Phys. Chem. C 2018, 122, 17118−17122